

# Eigenvalue spectrum of the survival probability of excitation in nonradiative energy transport

E.N. Bodunov<sup>a,1</sup>, M.N. Berberan-Santos<sup>a,\*</sup>, E.J. Nunes Pereira<sup>a,b</sup>,  
J.M.G. Martinho<sup>a</sup>

<sup>a</sup> *Centro de Química-Física Molecular, Instituto Superior Técnico, 1049-001 Lisboa, Portugal*

<sup>b</sup> *Dep. de Física, Escola de Ciências, Universidade do Minho, Campus de Gualtar, 4710-057 Braga, Portugal*

Received 19 January 2000

## Abstract

The eigenvalue spectrum of the initial excitation survival probability is computed for several models of nonradiative transport in current use. It is shown that the eigenvalue spectrum is more sensitive to the finer details of the models than the survival probability. In particular, short- and long-time behaviours are clearly displayed. Based on this analysis, a simple function for the survival probability is proposed. This function represents a numerical interpolation that combines the correct short- and long-time behaviour of different theories. Monte-Carlo simulations carried out for regular lattices in one, two and three dimensions allowed the accurate numerical computation of the respective eigenvalue distributions. © 2000 Elsevier Science B.V. All rights reserved.

## 1. Introduction

It is well known that concentration depolarization of luminescence in isotropic, rigid solutions occurs owing to resonance energy transfer (RET) [1]. Two types of RET are usually considered: radiative and nonradiative. Radiative transport was recently reviewed [2], and here, we will consider only the second type.

For nonradiative RET in isotropic media, only the radiation of molecules directly excited by a vertically polarized beam is significantly polarized. The luminescence of molecules subsequently excited by RET is almost completely depolarized [3]. Thus, for the quantitative description of luminescence anisotropy (and similar processes like the kinetics of fluorescence of rare-earth ions in solids studied by line-narrowing spectroscopy [4,5], or transport of spin polarization [6]), it is sufficient to focus attention on the survival probability function,  $G^s(t)$ . This function represents the average probability that an initially excited molecule is still excited at time  $t$ .  $G^s(t)$  reflects not only the first step of transfer, from molecules directly excited by light absorption to nearby ground state molecules, but also all subsequent multiple transfer paths by

\* Corresponding author.

*E-mail address:* berberan@ist.utl.pt (M.N. Berberan-Santos).

<sup>1</sup> On leave from Hydrometeorological University of Russia, 195196 St. Petersburg, Russian Federation.

which the excitation returns to the original molecule at a latter time. On the other hand,  $G^s(t)$  does not include the effect of the finite excited state lifetime, that if necessary, is accounted for by the factor  $\exp(-t/\tau)$ , where  $\tau$  is the excited state lifetime. The usefulness of the survival probability lies in its relationship with the luminescence anisotropy [7–9],  $r(t)$ . This quantity, defined for excitation with linear polarized light in the vertical direction by  $r(t) = (I_{\parallel}(t) - I_{\perp}(t))/(I_{\parallel}(t) + 2I_{\perp}(t))$ , where  $I_{\parallel}(t)$  is the luminescence intensity with vertical linear polarization measured at right angle, and  $I_{\perp}(t)$  is the luminescence intensity with horizontal linear polarization measured at right angle, is related to the survival probability by  $r(t) = r_0 G^s(t)$ , where  $r_0$  is the fundamental luminescence anisotropy, function of the excitation wavelength only.

## 2. Survival probability

Various theoretical methods have been employed to calculate the survival probability. Here, we briefly state the main results of the most accurate. Other methods are described in Refs. [5,10].

### 2.1. Gochanour–Andersen–Fayer method

The Gochanour–Andersen–Fayer (GAF) method [11] was used in Refs. [12–14]. In the three-particle approximation, it was obtained that

$$G_{\text{GAF}}^s(\bar{t}) = \exp\left[-\left(\frac{\pi^2}{32} - 0.1887\right)\bar{t}\right]f(\bar{t}),$$

$$f(\bar{t}) = \left(1 + \frac{\pi^2}{16}\bar{t}\right)\exp\left(\frac{\pi^2}{32}\bar{t}\right)\text{erfc}\left(\sqrt{\frac{\pi^2}{32}\bar{t}}\right) - \sqrt{\frac{\pi}{8}\bar{t}},$$

$$\bar{t} = c^2 t / \tau,$$

$$c = \frac{4}{3}\pi n R_0^3,$$
(1)

where  $n$  is the molecular concentration (number density),  $\tau$ , the excited-state lifetime, and  $R_0$ , the critical radius of RET for dipole–dipole (dd) interaction. An orientation-averaged dd interaction is assumed with the transfer rate between two molecules given by

$$w = \frac{1}{\tau} \left(\frac{R_0}{R}\right)^6,$$
(2)

$R$  being the intermolecular distance. In general, the orientation-dependent transfer rate needs to be considered [1,3,15,16]. When molecules in random solution are fixed in space on the time scale of RET,  $G^s(t)$  for the full transfer rate can be readily obtained from  $G^s(t)$  for the orientationally averaged rate [17].

The short-time expansion of Eq. (1) yields

$$G_{\text{GAF}}^s(\bar{t}) = 1 - \sqrt{\frac{\pi}{2}\bar{t}} + 0.8055\bar{t} - \dots, \quad \bar{t} \ll 1.$$
(3)

The numerical coefficients in Eq. (3) are exact. The value of the second one was confirmed in Ref. [18] (the value 0.8001 was obtained with an estimated error of about 0.7%).

## 2.2. Huber–Hamilton–Barnett method

Huber's approximation [19,20] (also called HHB method) is often used to calculate  $G^s(t)$ , owing to its simplicity and good accuracy. For the considered case, this approximation gives

$$G_H^s(\bar{t}) = \exp\left(-\sqrt{\frac{\pi}{2}\bar{t}}\right). \quad (4)$$

One obtains from Eq. (4) that for short times

$$G_H^s(\bar{t}) = 1 - \sqrt{\frac{\pi}{2}\bar{t}} + \frac{\pi}{4}\bar{t} - \dots. \quad (5)$$

The function given in Eq. (5) has coefficients close to those of Eq. (3). It is usually considered that Eq. (4) is valid for  $G^s(t) \geq 0.05$ . However, this is not always correct. In Appendix A, we show that, in the case of a one-dimensional lattice, Huber's approximation is valid in a much narrower time range.

## 2.3. Continuous-time random-walk method

The continuous-time random-walk method (CTRW) was also used to obtain the survival probability [21]. The result is

$$G_{\text{CTRW}}^s(\bar{t}) = \exp\left(-\sqrt{\pi\bar{t}}\right) - \left[1 - \exp\left(-\sqrt{\pi\bar{t}}\right)\right] \left[1 + \frac{1.93}{(0.79\pi\bar{t} + 3.62)^{1/2}}\right] \frac{1}{(0.79\pi\bar{t} + 3.62)^{3/2}}. \quad (6)$$

For short times, Eq. (6) reduces to

$$G_{\text{CTRW}}^s(\bar{t}) = 1 - \sqrt{\frac{\pi}{2}\bar{t}} + \frac{\pi}{2}\bar{t} - \dots, \quad \bar{t} \ll 1. \quad (7)$$

Now, the numerical coefficient of the second term of Eq. (7) greatly exceeds the exact one in Eq. (3). Therefore, this method is not appropriate for short times.

The long-time limit of  $G^s(t)$  cannot be easily estimated by the GAF or HHB methods, since these are essentially good short-time approximations. On the other hand, the CTRW theory can be used to estimate such long-time limit: From Eq. (6) one obtains the diffusion-like asymptotic form

$$G_{\text{CTRW}}^s(\bar{t}) = \frac{1}{n(4\pi D\bar{t})^{3/2}} = \frac{0.25576}{\bar{t}^{3/2}}, \quad \bar{t} \gg 1, \quad (8)$$

where  $D$  is the excitation energy diffusion constant. It is generally accepted that  $G^s(t)$  has indeed a diffusive character for long times as first obtained by Förster for a cubic lattice [22]. According to Ref. [10], the diffusive limit is observed for sufficiently long times, such that  $G^s(t) < 10^{-3}$ .

All applicable theories (GAF, CTRW) give the same expression for the diffusion constant

$$D = AR_0^2 c^{4/3} / \tau. \quad (9)$$

Only the theoretical value of the numerical coefficient  $A$  varies [5] from 0.12 to 0.428. Its experimental value is [23]  $A = 0.20 \pm 0.03$ . The most recent attempt to calculate the diffusion constant, based on a lattice model in combination with Monte-Carlo simulations [24], gives  $A = 0.40$ .

#### 2.4. An ad hoc survival probability

Here, we suggest the use of an ad hoc function for the survival probability that incorporates the best results of previous models. It coincides with the exact form (Eq. (3)) for short times, and for long times has a diffusion asymptotic character. The numerical coefficient  $A$  in Eq. (9) for the diffusion constant is chosen to be equal to 0.23. This value was obtained by Monte-Carlo simulations [5], by the modified GAF method [25], and coincides (within experimental error) with the experimental one [23]. The proposed function is

$$G^s(\bar{t}) = \frac{0.852}{(\bar{t} + 9.1)^{3/2}} + \left(1 - \frac{0.852}{9.1^{3/2}}\right) \exp\left(-\frac{\sqrt{\pi\bar{t}/2}}{1 - 0.852/9.1^{3/2}}\right) \\ = \frac{0.852}{(\bar{t} + 9.1)^{3/2}} + 0.968 \exp\left(-1.2934\sqrt{\bar{t}}\right). \quad (10)$$

It can be seen that the first term of Eq. (10) gives a diffusion asymptotic at long times with a correct diffusion constant (in accordance with Eqs. (8) and (9)), and that the second one ensures the correct temporal dependence (Eq. (3)) for short times.

#### 2.5. Cubic lattice

The random medium can also be modelled by a three-dimensional simple cubic lattice of molecules with nearest-neighbour intermolecular interaction (this model can be named effective media model, EM). The exact solution for the survival probability is known [26,27],

$$G_{EM}^s(t) = e^{-6w_0t} [I_0(2w_0t)]^3, \quad (11)$$

where  $I_0$  is the modified Bessel function,  $w_0$ , the nearest-neighbour interaction in the effective media. For dd interaction, we can write

$$w_0 = \frac{1}{\tau} \left(\frac{R_0}{\bar{R}}\right)^6, \quad (12)$$

where  $\bar{R}$  is the lattice's nearest-neighbour distance,  $\bar{R} = n^{-1/3}$ . Then,  $w_0\tau = (3/4\pi)^2 c = 0.057c$ , and we have from Eq. (11)

$$G_{EM}^s(\bar{t}) = \exp(-0.342\bar{t}) [I_0(0.144\bar{t})]^3. \quad (13)$$

This function has the following short- and long-time asymptotes

$$G_{EM}^s(\bar{t}) = 1 - 0.342\bar{t} + \dots, \quad \bar{t} \ll 1, \\ G_{EM}^s(\bar{t}) = \frac{1.64958}{\bar{t}^{3/2}}, \quad \bar{t} \gg 1. \quad (14)$$

The short-time asymptotic has a linear dependence on time because of the existence of a minimum (nearest neighbour) distance,  $\bar{R}$ .

The temporal dependences of  $G_{GAF}^s(\bar{t})$ ,  $G_H^s(\bar{t})$ ,  $G_{CTRW}^s(\bar{t})$ , and  $G_{EM}^s(\bar{t})$  are depicted in Fig. 1. One can see that the temporal dependences of  $G_{GAF}^s(\bar{t})$  and  $G_H^s(\bar{t})$  are practically identical in the time domain  $0 < \bar{t} < 10$ . Their major drawback is that they do not give a diffusion asymptotic at very long times (not shown).

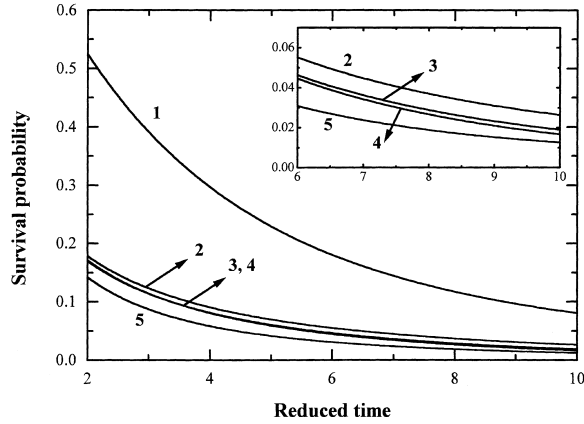


Fig. 1. Survival probability decay as a function of the reduced time defined in Eq. (1), computed according to (1) EM model, (2) ad hoc decay law, (3) HHB model, (4) GAF model, and (5) CTRW model.

### 3. Eigenvalue spectrum

In the past years, a different approach to the description and understanding of RET [9,25,28–30] was proposed. It is based on the fact that the survival probability can be expressed as the Laplace transform of some function  $F(k)$  (for details see the references cited),

$$G^s(\bar{t}) = \int_0^\infty F(k) \exp(-k\bar{t}) dk, \quad \int_0^\infty F(k) dk = 1. \quad (15)$$

This function (the inverse Laplace transform of the survival probability) has the meaning of an eigenvalue spectrum, and represents the set of eigenvalues  $k$  and respective contribution for the temporal behaviour of the survival probability. In particular, when the spectrum is discrete

$$F(k) = \sum_i f(k_i) \delta(k - k_i), \quad \sum_i f(k_i) = 1,$$

the survival probability is a sum of exponentials

$$G^s(t) = \sum_i f(k_i) \exp(-k_i t).$$

An equation of this type, containing only two or three terms, is often used to analyse experimental luminescence decays.

The function  $F(k)$  is well known for Huber's approximation [19,20]

$$F_H(k) = \frac{1}{2\sqrt{2}k^{3/2}} \exp\left(-\frac{\pi^2}{8k}\right). \quad (16)$$

We did not calculate the inverse Laplace transform of the survival probability for the GAF approximation,  $G_{\text{GAF}}^s(\bar{t})$ , since its time dependence is identical to that of  $G_H^s(\bar{t})$ .

By careful numerical calculations, an approximate inverse Laplace transform of  $G_{\text{CTRW}}^s(\bar{t})$  is obtained

$$F_{\text{CTRW}}(k) = 0.2886\sqrt{k} \exp(-1.2k) + \frac{1}{2\sqrt{2}k^{3/2}} \exp\left(-\frac{0.6053}{k}\right). \quad (17)$$

This function reproduces the survival probability in the CTRW approximation with a precision better than 0.5% at all times. The first term of Eq. (17) gives the diffusion kinetics (Eq. (8)) at long times, and the second one gives the HHB model at short times.

The ad hoc survival probability, Eq. (10), has the following analytical inverse Laplace transform

$$\begin{aligned} F(k) &= \frac{0.852}{\Gamma(3/2)} \sqrt{k} \exp(-9.1k) + \frac{1}{2\sqrt{2}k^{3/2}} \exp\left(-\frac{1.2934^2}{4k}\right) \\ &= 0.9614\sqrt{k} \exp(-9.1k) + \frac{1}{2\sqrt{2}k^{3/2}} \exp\left(-\frac{0.4182}{k}\right), \end{aligned} \quad (18)$$

whose two terms have the same meaning as in Eq. (17).

Again by careful numerical calculation, the approximate inverse Laplace transform of the survival probability in the EM approximation,  $F_{EM}(k)$ , can be obtained. The following information about this function was used: First,  $F_{EM}(k)$  obeys the normalization condition (15). Second, for small  $k$ , this function has to verify

$$F_{EM}(k) = \frac{1.64958}{\Gamma(3/2)} \sqrt{k} = 1.86135\sqrt{k} \quad (19)$$

in order to give the correct diffusion asymptotic (Eq. (14)) for long times. Third, the width of the spectrum of eigenvalues is limited from above by  $12w_0\tau/c = 12 \times 0.057$  (due to the existence of a minimum (nearest neighbour) distance,  $\bar{R}$ , see Appendix B for details) so

$$0 \leq k \leq 0.684. \quad (20)$$

Fourth, the eigenvalue spectrum is symmetric (this follows from the fact that the spectrum is related to the eigenvalue spectrum of the one-dimensional lattice, which is symmetric, see Appendix B). Thus, taking account of Eq. (19), we have for  $k \leq 0.684$

$$F_{EM}(k) = 1.86135\sqrt{0.684 - k}. \quad (21)$$

After fulfillment of the numerical calculations (comparing exact kinetics (13) with the calculated one from Eq. (15) in which the function  $F_{EM}(k)$  was modelled by an empirical one possessing enumerated properties), it was obtained that the following function

$$\begin{aligned} F_{EM}(k) &= \left( 1.86135 \left[ \sqrt{k} \frac{1 + \text{sign}(0.342 - k)}{2} + \sqrt{0.684 - k} \frac{1 - \text{sign}(0.342 - k)}{2} \right] \right. \\ &\quad \left. + 1.8091 \left\{ \exp \left[ - \left( \frac{k - 0.342}{0.162} \right)^2 \right] - \exp \left[ - \left( \frac{0.342}{0.162} \right)^2 \right] \right\} \right) \left( \frac{1 + \text{sign}(0.684 - k)}{2} \right) \end{aligned} \quad (22)$$

reproduces the survival probability  $G_{EM}^s(\bar{r})$  (Eq. (13)) with a precision better than 0.1%. Note that only one parameter (its final value is 0.162) was used in the fitting. In Eq. (22),  $\text{sign}(x)$  is equal to 1 if  $x > 0$  and  $-1$  if  $x < 0$ .

The eigenvalue spectra  $F_H(k)$ ,  $F_{CTRW}(k)$ ,  $F(k)$ , and  $F_{EM}(k)$  (Eqs. (16–19)) are depicted in Fig. 2. One can see significant differences between the first three spectra for low  $k$  values ( $k < 0.2$ ), corresponding to very long times. For  $k > 0.6$ , all practically coincide, with the exception of the EM model, in agreement with

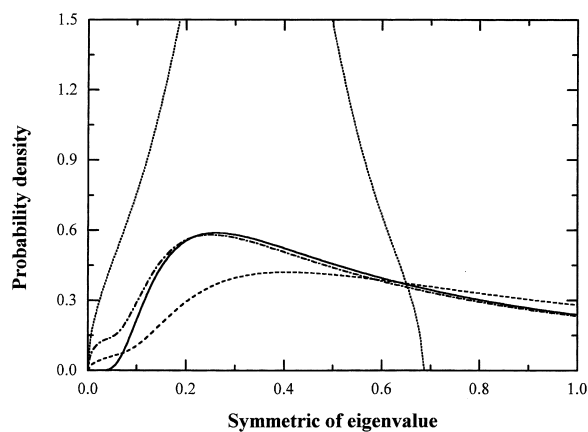


Fig. 2. Eigenvalue spectra for the different approximations: EM model ( $\cdots$ ), ad hoc decay law ( $-\cdot-\cdot-$ ), HHB model ( $-$ ), and CTRW model ( $- -$ ).

Fig. 1. The eigenvalue spectrum is, therefore, a very sensitive tool for the test of theories of nonradiative transport.

We next describe Monte-Carlo simulations for a regular lattice in one (evenly-spaced), two (square) and three (simple cubic) dimensions. Two situations are considered: Firstly, with nearest-neighbour interactions only; secondly, a more general case with all interactions allowed.

## 4. Monte-Carlo simulations in regular lattices

### 4.1. Simulation method

Two different models were considered. Interaction with nearest neighbours only, and interaction with all neighbours. The computation of the distribution of the symmetric of eigenvalues was made as follows. For each dimension, a periodic lattice was used in the construction of the Förster transfer rate matrix. Transfer matrix entries were always dimensionless, i.e., computed in terms of the nearest-neighbour rate transfer value. All the lattice sites were considered occupied and cubic type periodic boundary conditions were applied in each of the necessary dimension coordinates in parallel with the so-called minimum image convention [31]. Matrix entries  $k_{ij}$  were then in all cases the transfer rates from  $i$  to the nearest of all the possible periodic images of  $j$  lattice site in the simulation cell. These entries were considered zero for all but the nearest neighbour in each dimension in the case of the model with nearest-neighbours interaction. In the general case of interactions of each individual molecule with all the minimum periodic images of  $j$  lattices sites, all the matrix entries were nonzero to machine precision.

Given the Förster transfer rate matrix, its eigenvalues were computed using the digital extended math library (DXML) v3.3 for digital UNIX implementation of the dense eigenproblem solvers of LAPACK v2.0 [32,33]. The eigenvalues found for each lattice simulation cell were then distributed over a fixed number of bins and the probability density functions estimated as histograms in units of nearest-neighbour interaction. The histograms shown in Figs. 3 and 4 were obtained by accumulating  $\approx 4$  million eigenvalue values for each considered geometry in order to decrease the variance of the estimated values. To do so, a variable number of simulation cells were constructed corresponding to several sizes of the lattices in each one of the cartesian coordinates. The number of lattice sites ranged from 1000 to  $\approx 7000$  and several tests

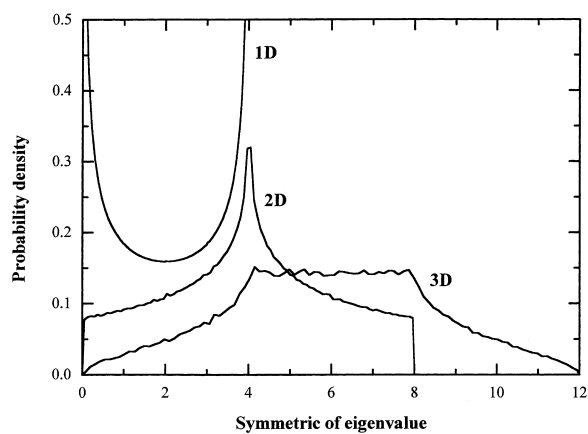


Fig. 3. Eigenvalue spectra, obtained by Monte-Carlo simulation, for regular lattices in one, two and three dimensions, considering only nearest-neighbour interactions.

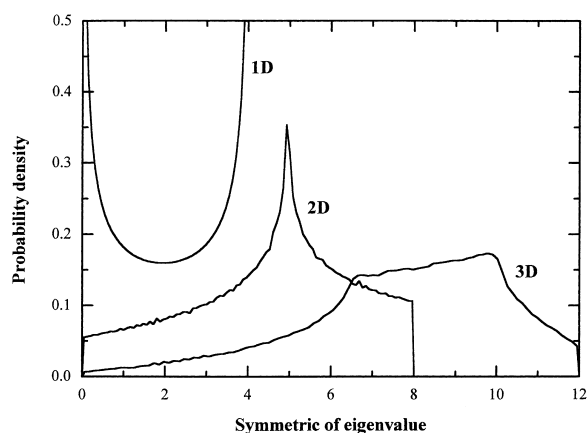


Fig. 4. Eigenvalue spectra, obtained by Monte-Carlo simulation, for regular lattices in one, two and three dimensions, considering interactions with all neighbours. Note the shift to higher values in two and three dimensions with respect to the results in Fig. 3.

were made in each case to ensure that sufficient sites existed in each dimension, so that the eigenvalues distribution found was independent on the simulation cell dimensions.

#### 4.2. Simulation results

The eigenvalue distributions computed for regular lattices with nearest-neighbour interaction only, depicted in Fig. 3, coincide with the exact analytical results given in Appendix B. When other neighbours are considered, the distributions become asymmetric, and are shifted towards higher values, as shown in Fig. 4. The noticeable shift to higher values in two dimensions and three dimensions, with respect to the results in Fig. 3, is due to the contribution of interactions with some neighbours other than the nearest that are still at a close distance. This contribution is negligible in one dimension, since second and higher order neighbours are always much more distant. In Appendix B, empirical functions are obtained for the eigenvalue distributions obtained by simulation.

## 5. Summary and conclusions

The survival probability functions computed from several models of nonradiative energy transport, including GAF, HHB, and CTRW, were compared. While the first two correctly describe the short-time behaviour, and fail for long times, the opposite happens with the CTRW model.

A systematic analysis of the eigenvalue spectra of models for radiative transport, carried out here for the first time, allows one to better discuss the finer details of the models than the survival probability, and is thus a better tool for their comparison. In particular, short- and long-time behaviours are clearly displayed.

Based on this analysis, a simple function for the survival probability in a random three-dimensional medium is proposed. This function represents a numerical interpolation, and combines the correct short- and long-time behaviour provided by different theories. Monte-Carlo simulations carried out for regular lattices in one, two and three dimensions allowed the accurate numerical computation of the respective eigenvalue distributions.

## Acknowledgements

E.N.B. was supported by an INVOTAN fellowship (ICCTI, Portugal). E.J.N.P. is grateful to Fundação Calouste Gulbenkian for financial support (Lisbon, Portugal) (Contract no. Est./Inv./96).

## Appendix A. HHB approximation in one dimension

Let us consider a linear and infinite chain of equally spaced molecules with nearest-neighbour interaction only (one-dimensional lattice). In this case, the survival probability,  $G_1^s(t)$ , is given by [26]

$$G_1^s(t) = e^{-2w_0 t} I_0(2w_0 t), \quad (\text{A.1})$$

where  $I_0$  is the modified Bessel function of zero order and  $w_0$ , the rate of RET between nearest-neighbour molecules.

Huber's approximation gives in this case for a dd interaction

$$G_{1H}^s(t) = \exp \left[ \sum_{n=1}^{\infty} 2 \ln \left( 1 + \frac{1}{2} e^{-2w_0 t/n^6} \right) \right]. \quad (\text{A.2})$$

One can see (Fig. 3) that Eqs. (A.1) and (A.2) coincide only if  $G_1^s(t) \geq 0.3$ . This condition differs significantly from the condition for three dimensions ( $G_1^s(t) \geq 0.05$ ) discussed in Section 2.2. The HHB method is, therefore, a poor approximation in one dimension.

## Appendix B. Eigenvalue distributions for regular lattices with nearest-neighbour interaction

The eigenvalue spectrum of a finite and closed unidimensional chain (containing  $N$  molecules) with nearest-neighbour interaction,  $w_0$ , was considered in Ref. [30]. This spectrum is discrete and the eigenvalues are given by (in  $w_0$  units)

$$k_n = 2 + 2(-1)^{n+1} \cos \left[ \frac{(N-2)n\pi}{N} \right], \quad n = 1, 2, \dots, N. \quad (\text{B.1})$$

Note that one eigenvalue (the smallest) is equal to zero ( $n = 0$  in Eq. (B.1)) because the survival probability in this case approaches a constant value  $1/N$  when  $t \rightarrow \infty$  (the excitation has equal probability to be at each

molecule). The largest eigenvalue is equal to  $4w_0$  if  $N$  is even or approaches this value when  $N$  is odd and large.

For an infinite unidimensional chain of molecules, the survival probability (A.1) can be rewritten as

$$G_1^s(\bar{t}) = \exp(-2\bar{t})I_0(2\bar{t}), \quad (\text{B.2})$$

where  $\bar{t} = w_0 t$ . The eigenvalue spectrum (the inverse Laplace transform,  $F_1(k)$ ) of Eq. (B.2) is well known. It is continuous, lies in the limited interval  $0 \leq k \leq 4$  and has symmetrical shape

$$F_1(k) = \frac{1}{\pi\sqrt{k(4-k)}}. \quad (\text{B.3})$$

Function (B.3) is shown in Fig. 3.

Let us now consider a two-dimensional molecular system formed by a finite square lattice of  $4 \times 4$  molecules with nearest-neighbour interaction,  $w_0$ . We suppose that molecules situated at the boundaries of this lattice interact with the molecules situated at the opposite boundaries with the same rate of RET,  $w_0$ . So these 16 molecules form a torus in three-dimensional space. In this case, the eigenvalue spectrum (in  $w_0$  units) is discrete and the eigenvalues are  $k = 8$  (one value),  $k = 6$  (four values),  $k = 4$  (six values),  $k = 2$  (four values) and  $k = 0$  (one value). So, the spectrum is symmetrical. Again (like in the one-dimensional finite lattice), one eigenvalue is equal to zero because the survival probability goes to the constant value  $1/16$  when  $t \rightarrow \infty$ . Note that the spectrum lies in the interval  $0 < k < 8$  which is two times larger the corresponding interval in one dimension.

The survival probability for an infinite two-dimensional lattice,  $G_2^s(\bar{t})$ , is well known [26]

$$G_2^s(\bar{t}) = [G_1^s(\bar{t})]^2 = \exp(-4\bar{t})[I_0(2\bar{t})]^2. \quad (\text{B.4})$$

At long times, it has the asymptotic form

$$G_2^s(\bar{t}) \xrightarrow{\bar{t} \rightarrow \infty} \frac{1}{4\pi\bar{t}} = \frac{0.0795775}{\bar{t}}. \quad (\text{B.5})$$

This means that the eigenvalue spectrum of Eq. (B.5) (inverse Laplace transform,  $F_2(k)$ ) is constant when  $k \rightarrow 0$ ,  $F_2(0) = 1/(4\pi)$ . Due to Eq. (B.4), spectrum  $F_2(k)$  can be expressed through  $F_1(k)$ . So, spectrum  $F_2(k)$  has to be symmetric (as  $F_1(k)$ ) and to be localized inside the interval  $0 < k < 8$  (see also the spectrum of finite two-dimension lattice). Thus, it has to be  $F_2(k=8) = 1/(4\pi)$ . Finally, the function  $F_2(k)$  is normalized (Eq. (15)) due to condition  $G_2^s(1) = 1$ . After some numerical calculations (carried out by comparing the exact kinetics (B.4) with those calculated with Eq. (15) in which the function  $F_2(k)$  was modelled by an empirical one having the enumerated properties), it was obtained that function

$$F_2(k) = \frac{1}{4\pi} + 0.1037 \left\{ \exp \left[ - \left( \frac{k-4}{2.123} \right)^2 \right] - \exp \left[ - \left( \frac{4}{2.123} \right)^2 \right] \right\} \quad (\text{B.6a})$$

reproduces the survival probability  $G_2^s(\bar{t})$  (Eq. (B.4)) with a precision  $< 1\%$ . Note that only one parameter (its final value is 2.123) was fitted.

Using the explicit results in  $k$  space obtained by Monte-Carlo simulation, one can observe that it is better to use another empirical distribution function. Indeed, the function

$$F_2(k) = \frac{1}{4\pi} + 0.242377 \left( \frac{1}{1.1 + |4-k|} - \frac{1}{1.1+4} \right) \quad (\text{B.6b})$$

reproduces the survival probability  $G_2^s(\bar{t})$  (Eq. (B.4)) with a higher precision ( $< 0.3\%$ ). Note that only one parameter (its final value is 1.1) was fitted.

Let us now consider a three-dimensional molecular system formed by a finite cubic lattice of  $4 \times 4 \times 4$  molecules with nearest-neighbour interaction,  $w_0$ . Again, we suppose that molecules situated at the boundaries of this lattice interact with the molecules situated at the opposite boundaries with the same rate of RET,  $w_0$ . So, these 64 molecules define a torus in four-dimensional space. In this case, the eigenvalue spectrum (in  $w_0$  units) is discrete and eigenvalues are given by  $k = 12$  (one value),  $k = 10$  (six values),  $k = 8$  (15 values),  $k = 6$  (20 values),  $k = 4$  (15 values),  $k = 2$  (six values), and  $k = 0$  (one value). So, the spectrum is symmetrical. Again (like in one and two-dimensional finite lattices), one eigenvalue is equal to zero because the survival probability goes to the constant value  $1/64$  when  $t \rightarrow \infty$ . Note that the spectrum  $F_2(k)$  lies in the interval  $0 < k < 12$  which in three times larger the corresponding interval in one dimension.

The survival probability for the infinite simple cubic lattice,  $G_3^s(\bar{t})$ , is well known [26,27]

$$G_3^s(\bar{t}) = [G_1^s(\bar{t})]^3 = \exp(6\bar{t})[I_0(2\bar{t})]^3. \quad (\text{B.7})$$

At long times, it has the asymptote

$$G_3^s(\bar{t}) \xrightarrow{\bar{t} \rightarrow \infty} \left( \frac{1}{\sqrt{4\pi\bar{t}}} \right)^3 = \frac{0.0224484}{\bar{t}^{3/2}}. \quad (\text{B.8})$$

The last equation means that the eigenvalue spectrum,  $F_3(k)$ , of survival probability (B.7) can be written for small  $k$  as

$$F_3(k) = \frac{1}{4\pi^2} \sqrt{k}, \quad k \ll 1. \quad (\text{B.9})$$

Due to Eq. (B.7), spectrum  $F_3(k)$  can be expressed through  $F_1(k)$ . So, spectrum  $F_3(k)$  has to be symmetric (as  $F_1(k)$ ) and to be localized inside the interval  $0 < k < 12$  (see also the spectrum of finite three-dimension lattice). Thus, at  $k \rightarrow 12$ , it has to be

$$F_3(k) = \frac{1}{4\pi^2} \sqrt{12 - k}. \quad (\text{B.10})$$

Finally, the function  $F_3(k)$  is normalized (Eq. (15)) due to condition  $G_3^s(1) = 1$ . After fulfillment of numerical calculation (comparing exact kinetics (B.7) with calculated one from Eq. (15) in which the function  $F_3(k)$  was modelled by an empirical one fulfilling the enumerated properties), it was obtained that function

$$F_3(k) = \frac{1}{4\pi^2} \left[ \sqrt{k} \frac{1 + \text{sign}(6 - k)}{2} + \sqrt{12 - k} \frac{1 - \text{sign}(6 - k)}{2} \right] + 0.10312 \left\{ \exp \left[ - \left( \frac{k - 6}{2.842} \right)^2 \right] - \exp \left[ - \left( \frac{6}{2.842} \right)^2 \right] \right\} \quad (\text{B.11a})$$

reproduces the survival probability  $G_3^s(\bar{t})$  (Eq. (B.7)) with a precision better than 1%. Note that only one parameter (its final value is 2.842) was fitted.

Using the explicit results in  $k$  space obtained by Monte-Carlo simulation, one can observe that again it is better to use another empirical distribution function. Indeed, the function

$$F_3(k) = \frac{1}{4\pi^2} \left[ \sqrt{k} \frac{1 + \text{sign}(6 - k)}{2} + \sqrt{12 - k} \frac{1 - \text{sign}(6 - k)}{2} \right] + 0.0048076 \left[ k^{1.82} \frac{1 + \text{sign}(4 - k)}{2} + (12 - k)^{1.82} \frac{1 - \text{sign}(8 - k)}{2} \right] + 0.14 \frac{\text{sign}(4 - k) + \text{sign}(8 - k)}{2} \quad (\text{B.11b})$$

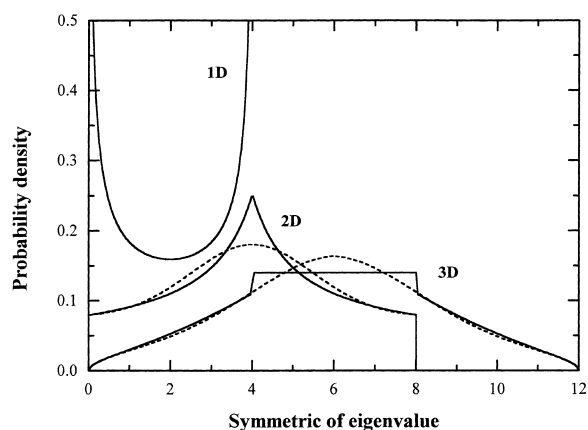


Fig. 5. Eigenvalue spectra for regular lattices in one, two and three dimensions, considering only nearest-neighbour interactions. The curves are the analytical approximations discussed in Appendix B. For two and three dimensions, functions  $a$  (---) and  $b$  (—) are shown. The spectra obtained by Monte-Carlo simulation are shown in Fig. 3.

reproduces the survival probability  $G_2^S(\bar{t})$  (Eq. (B.4)) with higher precision ( $< 0.3\%$ ). Note that only one parameter (its final value is 1.82) was fitted.

The connection between  $F_3(k)$  and  $F_{EM}(k)$  spectra (Eq. (22)) is determined by the equation

$$F_{EM}(k) = \frac{1}{0.057} F_3\left(\frac{k}{0.057}\right). \quad (\text{B.12})$$

The empirical functions  $F_1(k)$ ,  $F_2(k)$ , and  $F_3(k)$  and the respective eigenvalue spectra are depicted in Fig. 5.

## References

- [1] M.D. Galanin, *Luminescence of Molecules and Crystals*, CISP, Cambridge, 1996.
- [2] M.N. Berberan-Santos, E.J.N. Pereira, J.M.G. Martinho, in: D.L. Andrews, A.A. Demidov (Eds.), *Resonance Energy Transfer*, Wiley, New York, 1999.
- [3] M.N. Berberan-Santos, B. Valeur, *J. Chem. Phys.* 95 (1991) 8048.
- [4] T.T. Basiev, V.A. Malyshev, A.K. Przhnevskii, in: A.A. Kaplyanskii, R.M. MacFarlane (Eds.), *Spectroscopy of Solids Containing Rare-Earth Ions*, Elsevier, Amsterdam, 1987.
- [5] E.N. Bodunov, *Opt. Spectrosc.* 84 (1998) 350.
- [6] Yu.G. Abov, M.I. Bulgakov, S.P. Borovlev, A.D. Gul'ko, V.M. Garochkin, F.S. Dzheparov, S.V. Stepanov, S.S. Trostin, V.E. Shestopal, *Sov. Phys. JETP* 72 (1991) 534.
- [7] G.H. Frederickson, H.C. Andersen, C.W. Frank, *Macromolecules* 16 (1983) 1456.
- [8] A.H. Marcus, D.M. Hussey, N.A. Diachun, M.D. Fayer, *J. Chem. Phys.* 103 (1995) 8189.
- [9] M.N. Berberan-Santos, P. Choppinet, A. Fedorov, L. Jullien, B. Valeur, *J. Am. Chem. Soc.* 121 (1999) 2526.
- [10] P.T. Rieger, S.P. Palese, R.J.D. Miller, *Chem. Phys.* 221 (1997) 85.
- [11] C.R. Gochanour, H.C. Andersen, M.D. Fayer, *J. Chem. Phys.* 70 (1979) 4254.
- [12] B. Movaghar, G.W. Sauer, *J. Phys. C* 13 (1980) 4933.
- [13] S.G. Fedorenko, A.I. Burshtein, *Chem. Phys.* 98 (1985) 341.
- [14] E.N. Bodunov, V.A. Malyshev, *Sov. Phys. Solid State* 27 (1985) 2193.
- [15] B.W. van der Meer, in: D.L. Andrews, A.A. Demidov (Eds.), *Resonance Energy Transfer*, Wiley, New York, 1999.
- [16] A.A. Demidov, D.L. Andrews, in: D.L. Andrews, A.A. Demidov (Eds.), *Resonance Energy Transfer*, Wiley, New York, 1999.
- [17] C.R. Gochanour, M.D. Fayer, *J. Phys. Chem.* 85 (1981) 1989.
- [18] I. Rips, J. Jortner, *Chem. Phys.* 128 (1988) 237.

- [19] D.L. Huber, D.S. Hamilton, B. Barnett, *Phys. Rev. B* 16 (1977) 4642.
- [20] D.L. Huber, *Top. Appl. Phys.* 49 (1981) 83.
- [21] V.P. Gapontsev, F.S. Dzheparov, N.S. Platonov, V.E. Shestopal, *JETP Lett.* 41 (1985) 565.
- [22] Th. Förster, *Ann. Phys.* 2 (1948) 55.
- [23] L. Gomez-Jahn, J. Kasinski, R.J.D. Miller, *Chem. Phys. Lett.* 125 (1986) 500.
- [24] F.S. Dzheparov, D.V. L'vov, V.E. Shestopal, *Sov. Phys. JETP* 87 (1998) 1179.
- [25] B. Mollay and H.F. Kauffmann, in: R. Richert, A. Blumen (Eds.), *Disorder Effects on Relaxational Processes*, Springer, Berlin, 1994.
- [26] M.N. Barber, B.W. Ninham, *Random and Restricted Walks*, Gordon and Breach, New York, 1970.
- [27] R.F. Loring, H.C. Andersen, M.D. Fayer, *J. Chem. Phys.* 80 (1984) 5731.
- [28] A.K. Livesey, J.C. Brochon, *Biophys. J.* 52 (1987) 693.
- [29] B.D. Wagner, W. Ware, *J. Phys. Chem.* 94 (1990) 3489.
- [30] M.N. Berberan-Santos, J. Canceill, E. Gratton, L. Jullien, J.M. Lehn, P. So, J. Sutin, B. Valeur, *J. Phys. Chem.* 100 (1996) 15.
- [31] M.P. Allen, D.J. Tildesley, *Computer Simulation of Liquids*, Oxford University Press, Oxford, 1987.
- [32] Digital Extended Math Library for Digital UNIX reference manual.
- [33] E. Anderson, Z. Bai, C. Bischof, J. Demmel, J. Dongarra, J. Du Croz, A. Greenbaum, S. Hammarling, A. McKenney, S. Ostrouchov, D. Sorensen, *Lapack User's Guide*, second ed., SIAM, Philadelphia, 1995.